ELSEVIER

Fusion Engineering and Design 28 (1995) 708–715

Fusion Engineering and Design

Integral experiment on effects of large opening in fusion reactor blanket on tritium breeding using annular geometry

Chikara Konno [a], Yukio Oyama [a], Fujio Maekawa [a], Yujiro Ikeda [a], Kazuaki Kosako [a], Hiroshi Maekawa [a], M.A. Abdou [b], A. Kumar [b], M.Z. Youssef [b]

[a] *Department of Reactor Engineering, Tokai Research Establishment, Japan Atomic Energy Research Institute, Tokai-mura, Naka-gun, Ibaraki-ken 319-11, Japan*

[b] *Mechanical, Aerospace, and Nuclear Engineering Department, School of Engineering and Applied Science, University of California at Los Angeles, Los Angeles, CA 90024, USA*

Abstract

An experiment involving a simulated blanket with an opening has been performed using the line source and annular blanket system developed under the JAERI/USDOE collaborative programme in order to examine the effects of the opening on neutronics parameters such as the tritium-breeding ratio. The annular test assembly was rectangular in shape and consisted of a lithium oxide blanket covered with graphite and SS304 which simulated the graphite armour plate and first wall in a fusion device. A large opening (376 mm × 425.5 mm) was made in the middle of the test blanket. This opening simulated a neutral beam injector.

Tritium production rates and reaction rates were measured inside the blanket. Neutron spectra and reaction rates were also measured on the surfaces of both sides with and without the opening of the inner cavity. The opening decreased the number of low energy neutrons contained in the cavity and especially decreased ^{6}Li tritium production by 10% inside the blanket at the opposite side of the opening. The Monte Carlo code GMVP using the JENDL-3 nuclear data library predicted the measured nuclear parameters in the test blankets, such as the tritium production rate, to within 10% accuracy.

1. Introduction

In a realistic reactor many ports and ducts are required for functions such as plasma diagnostics, neutral beam injection (NBI), vacuum pumping and so on. These openings and holes, especially the large openings for NBI, will influence the nuclear parameters around the ports owing to leakage of neutrons and reduction of reflected neutrons. For example, a coverage factor for estimating the tritium-breeding ratio should take account of the opening effect. A simple area fraction has been used so far as a factor to obtain the tritium-breeding ratio in a whole reactor from local breeding ratios calculated by a one-dimensional code. Since a volumetric D–T neutron source is necessary in order to examine the effect which openings and holes have on the neutronics parameters, no neutronics experiment has been executed so far.

A pseudoline D–T neutron source and an annular test blanket were developed for the third phase (Phase-III) of the JAERI/USDOE collaborative programme on fusion blanket neutronics [1,2]. The pseudoline source

0920-3796/95/$09.50
SSDI 0920-3796(94)00277-0

was achieved by oscillating an annular test blanket which was rectangular in shape. It was experimentally clear that the characteristics of the pseudoline source are very similar to those of a stationary line source [3]. The nuclear performance of the annular test blanket with graphite armour was also examined [4]. The system consisting of the pseudoline source and annular test blanket is very suitable for testing the neutronics effects of an opening, since the neutron source is not a point and the shape of the blanket is similar to a torus. A neutronics integral experiment on the effects of a large opening was performed as the third step (Phase-IIIC) of Phase-III.

This paper mainly describes the experimental set-up, measuring techniques and experimental results. The effect of the opening on the neutronics parameters is discussed via a comparison between the measured data for the annular blanket with and without the opening. A calculation using the Monte Carlo code GMVP [5] and the Japanese Evaluated Nuclear Data Library JENDL-3 [6] is compared with the measured data. A comprehensive calculation benchmark using this experiment is reported separately [7].

2. Experimental arrangement

2.1. Pseudoline source

The experimental system was installed in the large irradiation room of the Fusion Neutronic Source (FNS) facility [8] of the Japan Atomic Energy Research Institute (JAERI). A pseudoline neutron source [1] was realized by the annular test blanket oscillating relative to the fixed D–T point source over a span of 2 m. This pseudoline source simulated part of a torus-shaped plasma. Two operational modes of the carriage deck, i.e. stepwise and continuous modes, were adopted in the experiment. In the stepwise mode the annular test blanket on the carriage deck was stopped every 50 or 100 mm over the 2 m length and the detector signals were collected during pauses as source-positionwise data. This mode was applied to on-line measuring techniques such as NE213 and Li glass scintillators and proton recoil gas proportional counters. In the continuous mode the test blanket moved back and forth continuously at a constant speed of 6.1 mm s^{-1}. The position of the carriage deck and the neutron yield were recorded every 10 s. This mode was applied to passive techniques such as activation foil measurements requiring high neutron fluence.

A cup-shaped tritium–titanium metal target with a long (2.3 m) drift tube was specially made for insertion into the annular test blanket. The target of 370 GBq tritium cooled by water was bombarded with a 0.1–2 mA, 350 keV deuteron beam. The absolute D–T neutron yields were monitored to within an accuracy of 3% by an associated α-particle-counting method [9].

2.2. Annular test assembly

The annular test assembly, which modelled part of a Tokamak fusion device, was formed by stacking lithium oxide (Li_2O) and lithium carbonate (Li_2CO_3) blocks as shown in Fig. 1. SS304 of 15 mm thickness and graphite of 25 mm thickness were placed inside the Li_2O region to simulate the first wall and armour respectively. An opening of size 376 mm × 425.5 mm was made in the middle of the test blanket and lined by SS304 15 mm thick. The side with the opening in the cavity was termed the "opening side". The side opposite the opening side was called the "normal side". This annular test assembly was set on a large carriage deck of size 3.4 m × 4 m which was moved on four rails by a computer-controlled servo-motor drive system. One experimental channel was installed horizontally at the opposite side of the opening in the assembly as shown in Fig. 1 in order to measure the tritium production rate, neutron flux and reaction rate inside the lithium oxide blanket.

3. Measurements

Measurements of tritium production rates and reaction rates were performed using the experimental channel. Reaction rate distributions and neutron spectra from a few keV to 1 MeV were also measured on the surfaces of both the opening and normal sides of the inner cavity.

Two pairs of ^{6}Li-enriched and ^{7}Li-enriched glass scintillators [10] were used in parallel to measure the tritium production rate of ^{6}Li. Three NE213 scintillation detectors [11] were operated simultaneously to measure the tritium production rate of ^{7}Li, with the spectrum weighting function method [12] being adopted to reduce the data-processing time. The stepwise operation mode of the line source was used for these detectors.

Neutron spectra from a few keV to 1 MeV were measured by two small proton recoil gas proportional counters (PRCs) [13] in the stepwise operation mode. The applied high voltage was varied continuously in a ramp shape during acquisition to reduce the times of measurement and data processing [14].

Reaction rates were obtained by the activation foil method using the continuous operation mode of the

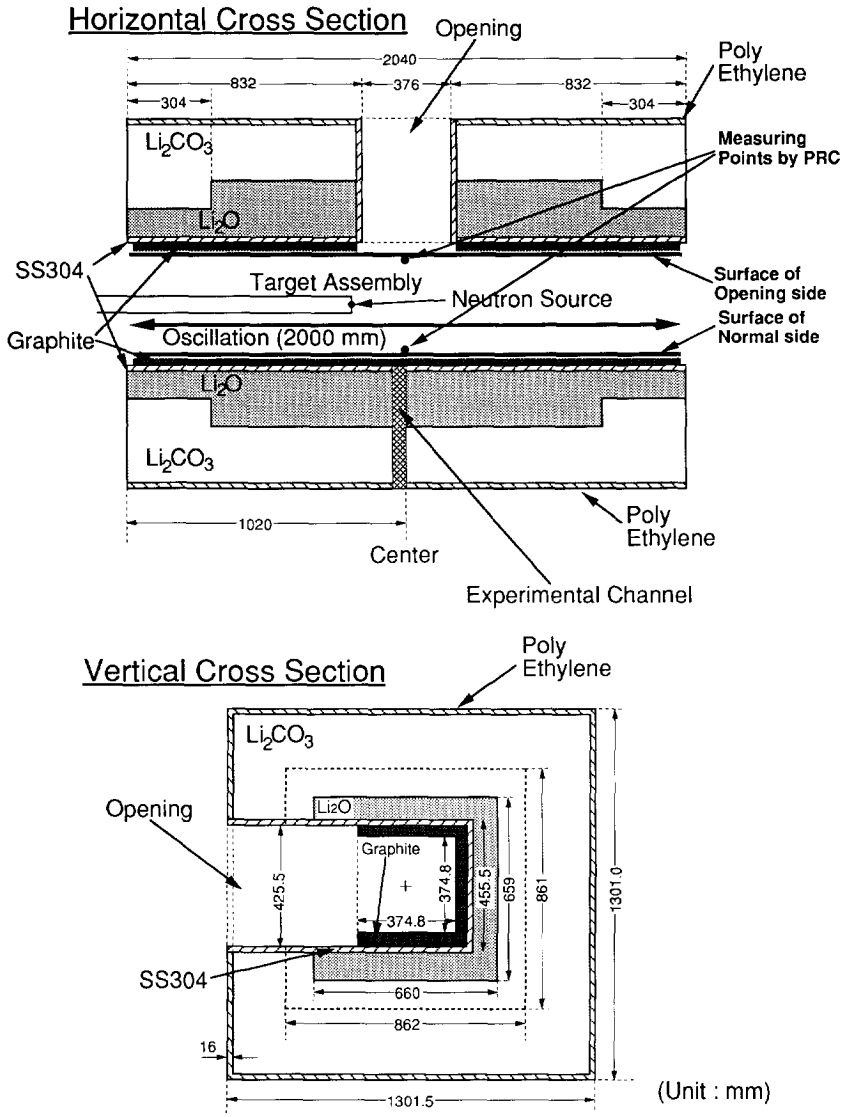

Fig. 1. Cross-sections of the large opening test blanket assembly.

line source. The activation reactions used were $^{27}Al(n, \alpha)^{24}Na$, $Ti(n, x)^{46}Sc$, $Ti(n, x)^{47}Sc$, $Ti(n, x)^{48}Sc$, $^{58}Ni(n, 2n)^{57}Ni$, $^{58}Ni(n, p)^{58}Co$, $^{64}Zn(n, p)^{64}Cu$, $^{90}Zr(n, 2n)^{89}Zr$, $^{93}Nb(n, 2n)^{92m}Nb$, $^{115}In(n, n')^{115m}In$ and $^{197}Au(n, \gamma)^{198}Au$. The foils, except gold, were 10–20 mm in diameter and 1 mm in thickness. A thin foil of 1 μm thickness was used for gold to avoid the self-shielding effect. γ Rays emitted from the irradiated foils were measured by four germanium detectors. A decay correction of activity [3] was performed by considering the fluctuations of movement speed and neutron yield in order to convert the measured data to the corresponding data for a stationary line source.

4. Results and discussion

The tritium production rates (TPRs) from ^{6}Li (T_6) and ^{7}Li (T_7) were measured separately by the Li glass and NE213 scintillators respectively. Both on-line methods (Li glass and NE213 scintillators) utilized the stepwise mode of the line source operation in order to

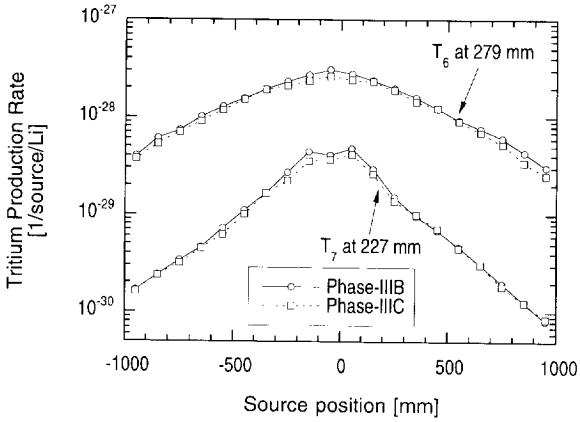

Fig. 2. T_6 profiles at 279 mm and T_7 profiles at 227 mm from the source travelling line in the experimental channel for the non-opening blanket (Phase-IIIB) and the opening blanket (Phase-IIIC).

obtain the source-positionwise tritium production rates T_6 and T_7 (termed the T_6 and T_7 profiles respectively). Fig. 2 shows the T_6 profiles at a distance of 279 mm and the T_7 profiles at a distance of 227 mm from the source travelling line in the experimental channel for the non-opening blanket (Phase-IIIB) [4] and the opening blanket (Phase-IIIC). The T_6 profiles are broader than those of T_7, because the T_6 profile is not dominated by an inverse square law of the distance from the target. The width of the T_6 profile is twice that of the T_7 profile. Comparing the opening blanket (Phase-IIIC) with the non-opening blanket (Phase-IIIB), T_6 and T_7 decrease by 10% only in a region comparable with the opening size, in contrast with the ^{197}Au(n, γ) reaction where the effect spreads over the cavity along the whole line source, as discussed later.

T_6 and T_7 for the line source were reduced by superposing the source profile data. The results in the experimental channel are shown in Fig. 3. T_7 decreases by 8% only in the front region, while T_6 decreases by 10% even at a depth of 193 mm owing to the opening.

Neutron spectra from a few keV to 1 MeV were measured by the PRCs in the stepwise line source mode. The measurements were performed at the centres of the surfaces of the opening and normal sides of the inner cavity. The data were taken every 100 mm step of the source position. The integrated neutron flux data from 10 keV to 1 MeV for each source-pointwise spectrum at the surfaces of the opening and normal sides of the inner cavity are shown in Fig. 4. This figure indicates that neutrons from 10 keV to 1 MeV at the opening side are fewer than those at the normal side by

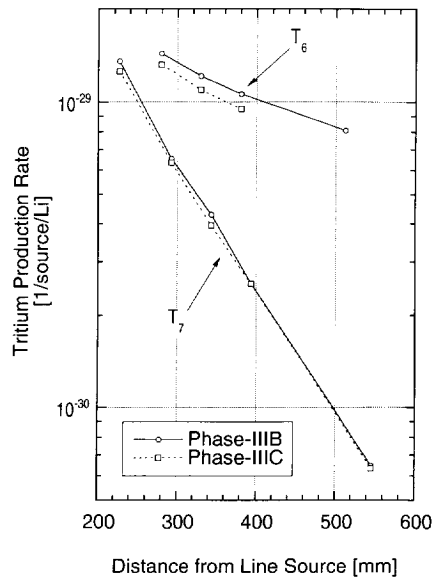

Fig. 3. Radial distributions of TPRs of ^{7}Li (T_7) and ^{6}Li (T_6) measured by NE213 and Li glass detectors in the experimental channel for Phase-IIIB and Phase-IIIC.

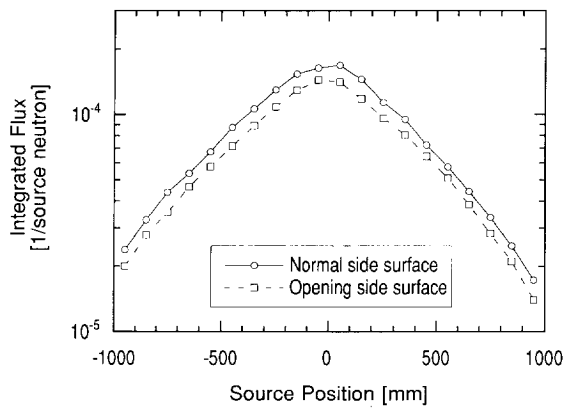

Fig. 4. Source-positionwise neutron flux profiles from 10 keV to 1 MeV measured by PRCs on the graphite surface of the opening and normal sides for Phase-IIIC.

about 20%, because there are no neutrons reflected from the graphite armour at the opening side.

Measurements of reactions rates by the activation foil method were performed in two directions: along the line source axis on the cavity surfaces of both the normal and opening sides and along the radial axis using the experimental channel.

The reaction rates of ^{93}Nb(n, 2n)^{92m}Nb, ^{115}In(n, n')^{115m}In and ^{197}Au(n, γ)^{198}Au were adopted as typical,

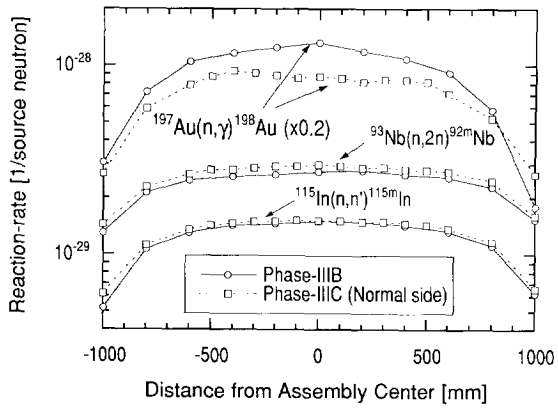

Fig. 5. Activation reaction rate distributions of ^{93}Nb(n, 2n)^{92m}Nb, ^{155}In(n, n')^{115m}In and ^{197}Au(n, γ)^{198}Au along the line source at the test region surface for Phase-IIIB and Phase-IIIC.

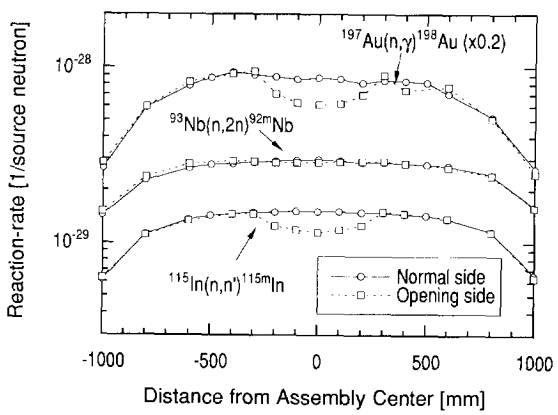

Fig. 6. Distributions of reaction rates of ^{93}Nb(n, 2n)^{92m}Nb, ^{115}In(n, n')^{115m}In and ^{197}Au(n, γ)^{198}Au on the graphite surface of the opening and normal sides for Phase-IIIC.

since the threshold values of these reactions are 9 MeV, 335 keV and zero respectively. Fig. 5 shows the measured reaction rate distributions along the line source at the surface of the inner cavity for Phase-IIIB and Phase-IIIC (normal side). The reaction rate of ^{197}Au(n, γ)^{198}Au decreases by 35% in the centre region owing to the opening effect. It is noted that the opening effect spreads over the cavity, in contrast with the tritium production rate of ^{6}Li. Fig. 6 shows the measured reaction rate distributions along the line source on both the opening and normal sides of the opening blanket (Phase-IIIC) surfaces. For ^{93}Nb(n, 2n)^{92m}Nb (high threshold reaction) there is no significant difference between the two sides of the surfaces, while for

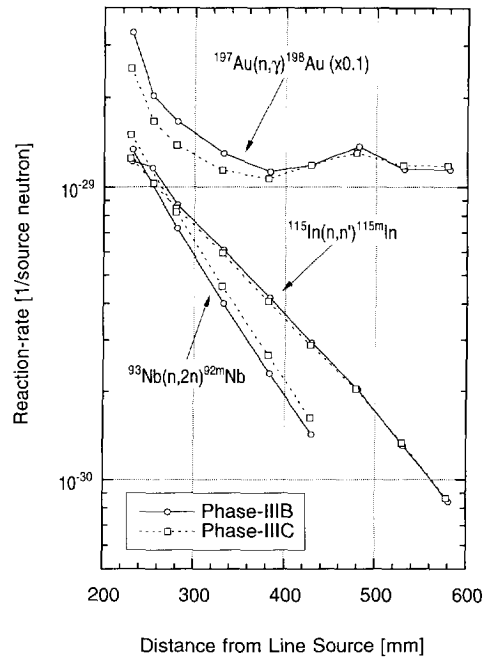

Fig. 7. Radial distributions of activation reaction rates of ^{93}Nb(n, 2n)^{92m}Nb, ^{115}In(n, n')^{115m}In and ^{197}Au(n, γ)^{198}Au in the experimental channel for Phase-IIB and Phase-IIIC.

^{115}In(n, n')^{115m}In and ^{197}Au(n, γ)^{198}Au a decrease in the reaction rate is clearly observed in the region corresponding to the width of the opening.

The reaction rate radial distributions of ^{93}Nb(n, 2n)^{92m}Nb, ^{115}In(n, n')^{115m}In and ^{197}Au(n, γ)^{198}Au in the experimental channel for Phase-IIIB and Phase-IIIC are plotted in Fig. 7. The reaction rates for ^{93}Nb(n, 2n)^{92m}Nb and ^{115}In(n, n')^{115m}In decrease monotonically with the depth. There is not much difference between the test blankets with and without the opening. The 10% difference in the reaction rate of ^{93}Nb(n, 2n)^{92m}Nb is probably due to some unconsidered experimental errors, since the reaction rate of ^{93}Nb(n, 2n)^{92m}Nb for Phase-IIIB cannot be smaller than that for Phase-IIIC. In contrast, the gold capture reaction distribution is almost flat and the gold reaction rate is lower than that for the test blanket without the opening (Phase-IIIB) even at a depth of 200 mm. This is due to a decrease in the reflected component (lower energy neutrons) from the opening side.

The Monte Carlo code GMVP [5] was adopted for the experimental analysis, since the shape of the experimental assembly was three dimensional. This code is a vectorized version of the Monte Carlo code MORSE-DD [15] using a multigroup double-differential cross-section

library. Because the computation speed of this vectorized version on a FACOM VP-2600 computer is 20 times faster than the scalar version, it is possible to obtain reliable calculation results for large experimental assemblies such as in the present experiment. The DDXLIB-J3 [16] nuclear data library of 125 groups was processed from JENDL-3.1 [6]. The line source was generated by random sampling of a point source with uniform probability over the source length. The track length estimators were placed at the measurement positions. The neutron history was 13 000 000 and the computing time was about 1.5 h.

The tritium production rates measured by Li glass and NE213 in the experimental channel of Phase-IIIC are compared with the calculated ones in Fig. 8. The calculated T_7 distribution underestimates the measured one by less than 10%.

Figs. 9 and 10 show comparisons of the measured and calculated reaction rates of ^{93}Nb(n, 2n)^{92m}Nb, ^{115}In(n, n′)^{115m}In and ^{197}Au(n, γ)^{198}Au on the surfaces of the opening and normal sides of the inner cavity for Phase-IIIC respectively. The calculations agree with the measured reaction rates of ^{93}Nb(n, 2n)^{92m}Nb and ^{115}In(n, n′)^{115m}In to within 10%. Although the large statistical error of the calculation for the reaction rate of ^{197}Au(n, γ)^{198}Au makes it difficult to discuss quantitatively, the trends are similar between the measured and calculated values.

The calculations also yield good agreement (within 10%) with the measured threshold reaction rates along the radial direction as shown in Fig. 11, while the discrepancy is more than 20% for the reaction rate of ^{197}Au(n, γ)^{198}Au. The tendency for the high threshold reactions is similar to the T_7 distributions.

Overall, the Monte Carlo code GMVP calculations with JENDL-3.1 agreed with the measured reaction rates

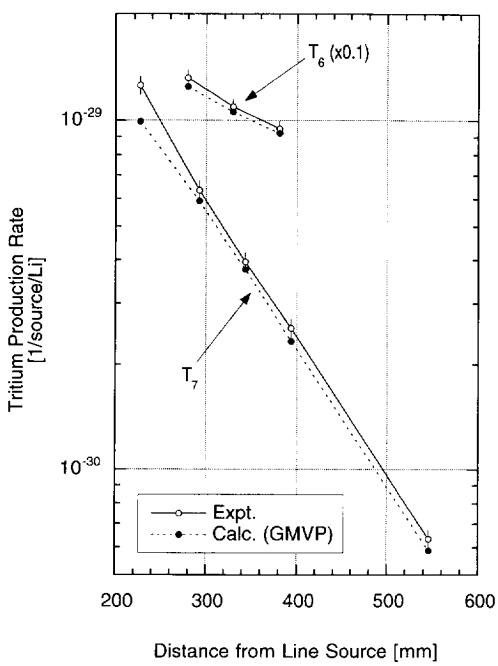

Fig. 8. Comparison between measured and calculated TPRs of ^{7}Li (T_7) and ^{6}Li (T_6) in the experimental channel for Phase-IIIC.

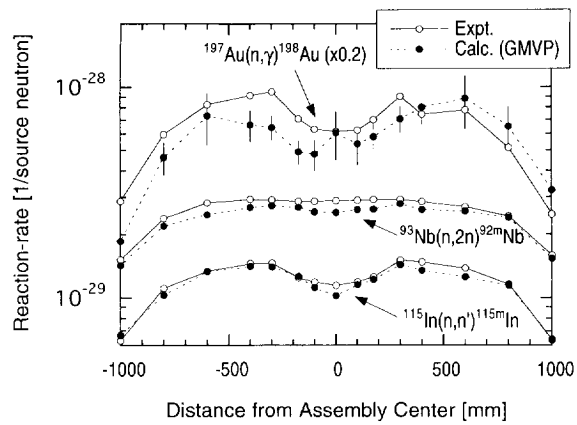

Fig. 9. Comparison between measured and calculated activation reaction rates of ^{93}Nb(n, 2n)^{92m}Nb, ^{115}In(n, n′)^{115m}In and ^{197}Au(n, γ)^{198}Au at the surface of the opening side of the inner cavity for Phase-IIIC.

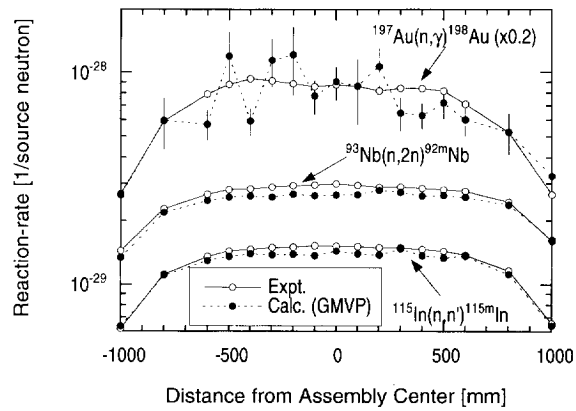

Fig. 10. Comparison between measured and calculated activation reaction rates of ^{93}Nb(n, 2n)^{92m}Nb, ^{115}In(n, n′)^{115m}In and ^{197}Au(n, γ)^{198}Au at the surface of the normal side of the inner cavity for Phase-IIIC.

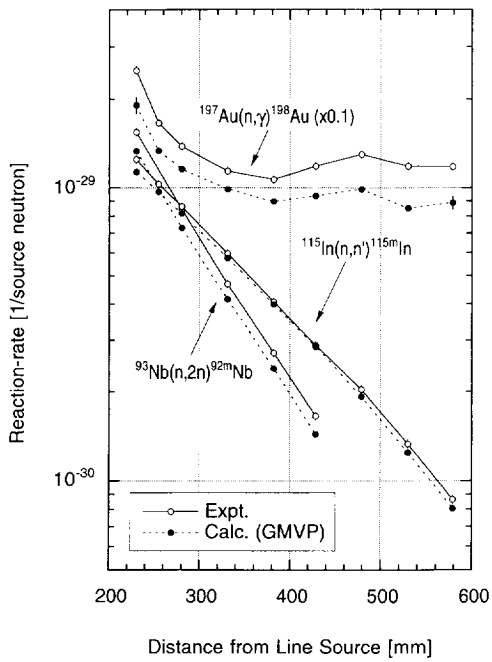

Fig. 11. Comparison between measured and calculated activation reaction rates of ^{93}Nb(n, 2n)^{92m}Nb, ^{115}In(n, n')^{115m}In and ^{197}Au(n, γ)^{198}Au in the experimental channel for Phase-IIIC.

and tritium production rates to within 10% in spite of a very complicated blanket configuration.

5. Concluding remarks

The effects of a large opening on neutronics parameters such as the tritium-breeding ratio have been examined using a pseudoline source of 2 m length and an annular blanket. The annular blanket was rectangular in shape and a test blanket configuration with a large opening at the center was used.

Tritium production rates, activation reaction rates and neutron spectra were measured inside the test blanket and/or along the line source at the surfaces of both sides with and without the opening of the inner cavity. The comparison between the experimental results for the test blankets with and without the opening suggested that the opening decreased the tritium production rate of ^{6}Li inside the test blanket by 10%. The Monte Carlo code GMVP using the JENDL-3.1 nuclear data library predicted the measured nuclear parameters in the test blankets, such as the tritium production rate, to within 10% accuracy.

Acknowledgment

The US work was supported by the US Department of Energy, Office of Fusion Energy.

References

[1] T. Nakamura, Y. Oyama, Y. Ikeda, C. Konno, H. Maekawa, K. Kosako, M.Z. Youssef and M.A. Abdou, A line D–T neutron source facility for annular blanket experiment: Phase-III of the JAERI/USDOE collaborative program on fusion neutronics, Fusion Technol. 19 (1991) 1873–1878.

[2] Y. Oyama, C. Konno, Y. Ikeda, H. Maekawa, K. Kosako, T. Nakamura, A. Kumar, M.Z. Youssef, M.A. Abdou and E.F. Bennett, Annular blanket experiment using a line DT neutron source: Phase-IIIA of the JAERI/USDOE collaborative program on fusion neutronics, Fusion Technol. 19 (1991) 1879–1884.

[3] C. Konno, Y. Oyama, Y. Ikeda, K. Kosako, H. Maekawa, T. Nakamura, A. Kumar, M.Z. Youssef, M.A. Abdou and E.F. Bennett, Measurements of the source term for annular blanket experiment with a line source: Phase-IIIA of the JAERI/USDOE collaborative program on fusion neutronics, Fusion Technol. 19 (1991) 1885–1890.

[4] Y. Oyama, C. Konno, Y. Ikeda, H. Maekawa, F. Maekawa, K. Kosako, T. Nakamura, A. Kumar, M.Z. Youssef, M.A. Abdou and E.F. Bennett, Phase-III experimental results of JAERI/USDOE collaborative program on fusion neutronics, Fusion Eng. Des. 18 (1991) 203–208.

[5] T. Mori, M. Nakagawa and M. Sasaki, Vectorized of continuous energy Monte Carlo method for neutron transport calculation, J. Nucl. Sci. Technol. 29 (1992) 325–336.

[6] K. Shibata, T. Nakagawa, T. Asami, T. Fukahori, T. Narita, S. Chiba, M. Mizumoto, A. Hasegawa, Y. Kikuchi, Y. Nakajima and S. Igarasi, JENDL-3: Japanese Evaluated Nuclear Data Library, Version-3, JAERI-1319, 1990.

[7] M.Z. Youssef, M.A. Abdou, A. Kumar, K. Kosako, Y. Oyama, F. Maekawa, Y. Ikeda, C. Konno and H. Maekawa, Analysis of fusion integral experiments on a Li_2O annular blanket system of various configurations surrounding a 14 MeV simulated line source, Fusion Eng. Des. 28 (1995).

[8] T. Nakamura, H. Maekawa, Y. Ikeda and Y. Oyama, A D–T neutron source for fusion neutronics experiments at the JAERI, Proc. Int. Ion Engineering Congr.—ISIAT '83 and IPAT '83, Kyoto, 1983, pp. 567–570.

[9] H. Maekawa, Y. Ikeda, Y. Oyama, S. Yamaguchi and T. Nakamura, Neutron yield monitors for the Fusion Neutronics Source (FNS), JAERI-M-83-219, 1983.

[10] S. Yamaguchi, Y. Oyama, T. Nakamura and H. Maekawa, An on-line method for tritium production measurement with a pair of lithium-glass scintillators, Nucl. Instrum. Methods A 254 (1987) 413–418.

[11] Y. Oyama, S. Tanaka, K. Tsuda, Y. Ikeda and H. Maekawa, A small spherical NE213 scintillation detector for use in in-assembly fast neutron spectrum measurements, Nucl. Instrum. Methods A 256 (1987) 333–338.

[12] Y. Oyama, K. Sekiyama and H. Maekawa, Spectrum weighting function method for in-situ fast neutron and gamma-ray response measurements in fusion integral experiments with an NE213 scintillation detector, Fusion Technol., in press.

[13] E.F. Bennett and T.J. Yule, Techniques and analyses of fast reactor neutron spectroscopy with proton-recoil proportional counters, ANL-7763, 1971.

[14] E.F. Bennett, A continuous mode data acquisition technique for proton recoil proportional counter neutron spectrometers, ANL/FPP/TM-239, 1989.

[15] M. Nakagawa and T. Mori, MORSE-DD, a Monte Carlo code using double differential form cross sections, JAERI-M 84-126, 1984.

[16] T. Mori, personal communication.